JOURNAL OF MATERIALS SCIENCE 30 (1995) 3177–3182

A micromechanics model of creep deformation in dispersion-strengthened metals

M. TANAKA
Department of Mechanical Engineering, Mining College, Akita University, 1-1 Tegatagakuen-cho, Akita 010 Japan

A micromechanics model, in which work-hardening caused by second-phase particles and a recovery process by diffusion of atoms were taken into account, has been proposed for explaining the creep deformation of dispersion-strengthened metals in high-temperature creep. A constitutive equation of the Θ projection was employed to describe the whole creep curves from the onset of loading to rupture. The results of the calculations based on the present model have been compared with those of experiments on the carbon steels containing spherical cementite particles. There was a correlation between the experimental creep curves and the calculated ones. The changes in the calculated creep strain and creep rate with time have also been compared with the experimental results on carbon steels. The micromechanics model was found to be applicable to any kind of two-phase material, if the constitutive equation was appropriately chosen.

1. Introduction

Creep curves of metallic materials are often characterized by three creep terms, namely, transient creep, steady-state creep and accelerated creep at high temperatures [1], but the creep deformation of a specimen does not always exhibit steady-state creep, or accelerated creep occupies most of the creep period in some kinds of material under certain creep conditions [2]. In these materials, the present structural design concept, which is based on the creep deformation up to steady-state creep, cannot be applied to the design and safety assurance of high-temperature structures. The Θ projection concept recently proposed [2], is a convenient method to reproduce the whole creep curves from the onset of loading to the rupture of specimens by a single equation. This method has been applied to the analysis of creep deformation in several kinds of metallic materials and ceramics [2, 3]. We [4] have analysed the creep deformation in the ductile two-phase alloys using a continuum mechanics model in which the internal stresses arising from the creep strain difference between the second phase and the matrix were taken into account. A similar creep model in which the Θ projection was incorporated as the constitutive equation, has also been applied [5] to the prediction of the creep deformation and rupture life, and a good correlation was found between the results of the analysis and the experimental results on ferrite–pearlite steels.

In precipitation-hardened or particle dispersion-strengthened metals and alloys, the strengthening phase generally does not creep and the creep deformation is controlled by the recovery process by diffusion of atoms around strong particles [6]. In this study, a micromechanics model was proposed, in which the Θ projection was employed as the constitutive equation and the diffusional recovery causing the decrease in the internal stresses in the strong second-phase particles was also taken into account. Creep curves of the matrix (ferrite) phase without second-phase (cementite) particles were simulated by the Θ projection. The simulated creep curves implicitly involve the microstructural effects, such as cavitation and back stresses, in the ferrite matrix. However, the internal stresses induced by the second phase generally depend not only on the material properties of the second phase and matrix but also on the current creep strain and creep strain rate of both phases, the applied stress, time and so on [4, 5], and can be affected by the diffusional recovery around the second-phase particles [7], although the second-phase particles are assumed to be non-deforming in this study. Therefore, the effects of the matrix properties and those of the internal stresses relating to the second-phase particles on the creep deformation were separately treated in this study. The results of the analysis based on this model were then compared with the results of the creep–rupture tests on carbon steels containing spherical cementite particles.

2. Stress and creep strain

Let us consider the creep deformation of a material containing non-deforming second-phase particles of ellipsoidal shape ($(x_2^1 + x_2^2)/a^2 + x_3^2/c^2 \leqslant 1$ in (x_1, x_2, x_3) co-ordinate) and of volume fraction of f, which are uniformly dispersed in the ductile matrix phase. It is assumed that both phases are elastically isotropic and the matrix is plastically isotropic. It is also assumed that creep strains are uniform in the matrix phase,

0022–2461

namely, $\varepsilon'_{33} = -2\varepsilon'_{11} = -2\varepsilon'_{22} = \varepsilon'$ under an applied tensile stress, σ^{A}_{33} (ε' is the equivalent creep strain of the matrix). In the present case, the diffusional recovery around the second-phase particles should be taken into account [7]. The virtual misfit strains between second-phase particles and matrix are $\varepsilon^{*}_{33} = -2\varepsilon^{*}_{11} = -2\varepsilon^{*}_{22} = \varepsilon^{*}$ (ε^{*} is the equivalent misfit strain between second-phase particles and the matrix), and ε^{*} is reduced to ε' when no recovery occurs. The components of internal stresses averaged over the matrix, σ^{I}_{ij}, and those averaged over the second phase, σ^{II}_{ij}, can be calculated by Eshelby's equivalent inclusion method [8–10] and Mori and Tanaka's average internal stress concept [11] and are expressed as [4]

$$\sigma^{I}_{33} = -fAE\varepsilon^{*}_{33} = -fAE\varepsilon^{*} \quad (1a)$$

$$\sigma^{I}_{11} = \sigma^{I}_{22} = fBE\varepsilon^{*}_{33} = fBE\varepsilon^{*} \quad (1b)$$

$$\sigma^{II}_{33} = (1-f)AE\varepsilon^{*} \quad (2a)$$

$$\sigma^{II}_{11} = \sigma^{II}_{22} = -(1-f)BE\varepsilon^{*} \quad (2b)$$

where E is Young's modulus of the matrix ($E = 2\mu(1+\nu)$, μ is the rigidity, and ν the Poisson's ratio). A and B are functions of Eshelby's tensor [9, 10, 12, 13], elastic moduli of the matrix phase (E, μ and ν) and those of the second phase (E^{*}, μ^{*} and ν^{*}). The actual stress acting on each phase and the equivalent stress, σ_e, are [4]

$$\sigma^{A}_{33} + \sigma^{I}_{33} = \sigma^{A}_{33} - fAE\varepsilon^{*} \quad (3a)$$

$$\sigma^{I}_{22} = \sigma^{I}_{11} = fBE\varepsilon^{*} \quad (3b)$$

$$\sigma^{I}_{e} = (1/2^{1/2})\{(\sigma^{I}_{11} - \sigma^{I}_{22})^2 + [\sigma^{I}_{22} - (\sigma^{A}_{33} + \sigma^{I}_{33})]^2 + [(\sigma^{A}_{33} + \sigma^{I}_{33}) - \sigma^{I}_{11}]^2\}^{1/2} = \sigma^{A}_{33} - f(A+B)E\varepsilon^{*} = \sigma^{A}_{33} - fKE\varepsilon^{*} \quad (3c)$$

for the matrix, and

$$\sigma^{A}_{33} + \sigma^{II}_{33} = \sigma^{A}_{33} + (1-f)AE\varepsilon^{*} \quad (4a)$$

$$\sigma^{II}_{22} = \sigma^{II}_{11} = -(1-f)BE\varepsilon^{*} \quad (4b)$$

$$\sigma^{II}_{e} = (1/2^{1/2})\{(\sigma^{II}_{11} - \sigma^{II}_{22})^2 + [\sigma^{II}_{22} - (\sigma^{A}_{33} + \sigma^{II}_{33})]^2 + [(\sigma^{A}_{33} + \sigma^{II}_{33}) - \sigma^{II}_{11}]^2\}^{1/2} = \sigma^{A}_{33} + (1-f)KE\varepsilon^{*} \quad (4c)$$

for the second phase, where $K(=A+B)$ is a shape factor. The value of shape factor K is $(7-5\nu)/[10(1-\nu^2)]$ for the spherical second phase of the same elastic moduli as those of the matrix [8]. The value of ε^{*} can be calculated by integrating the following equation with respect to time, t

$$d\varepsilon^{*}/dt = d\varepsilon' - C\varepsilon^{*} \quad (5)$$

where C is a factor relating to diffusional recovery, and is given by $3F\mu\Omega DS/(kTLV)$ [7]. F is a shape factor of second-phase particles and $(7-5\nu)/[5(1-\nu)]$ for the spherical second-phase particles of the same elastic moduli as those of the matrix, Ω is the atomic volume, D is a diffusion coefficient, S is the total cross-section of diffusion, L is the average diffusion distance of atoms, V is the volume of a second-phase particle, k is Boltzmann's constant and T is the absolute temperature. The average creep strain of the material, ε_{ij}, is expressed as

$$\varepsilon_{ij} = (1-f)\varepsilon'_{ij} \quad (6)$$

where the equivalent creep strain, ε, of the material is equal to ε_{33}. The internal stress distribution may occur in the second-phase particles owing to diffusional recovery [14, 15], but for simplicity the effects of the stress distribution were neglected in this study.

3. Constitutive equation

The creep deformation of a material containing strong second-phase particles at a current time, t, can be calculated on the basis of the micromechanics model, in which the internal stresses in both second phase and matrix caused by creep deformation of the matrix phase and the effects of diffusional recovery are taken into account.

If the creep deformation of the matrix phase is expressed by the constitutive equation of the Θ projection [2], the equivalent creep strain of the matrix, ε', is given by the following equation

$$\varepsilon' = \theta_1[1-\exp(-\theta_2 t)] + \theta_3[\exp(\theta_4 t) - 1] \quad (7)$$

$$\log_e\theta_i = a_i + b_i T + c_i\sigma^{I}_{e} + d_i\sigma^{I}_{e}T \quad (8)$$

where a_i, b_i, c_i and d_i ($i = 1$–4) are materials constants. The equivalent creep rate of the matrix, $d\varepsilon'/dt$, is given by [2]

$$d\varepsilon'/dt = \theta_1\theta_2\exp(-\theta_2 t) + \theta_3\theta_4\exp(\theta_4 t) \quad (9)$$

If the creep experiments are carried out at a constant temperature, the values of θ_i are given by

$$\log_e\theta_i = \alpha_i + \beta_i\sigma^{I}_{e} \quad (10)$$

where the materials constants, α_i and β_i ($i = 1$–4) should be obtained by the creep experiments. Putting Equation 10 into Equation 5 and integrating Equation 5 with respect to time, t, from $t = 0$–t, one can find the internal stresses and creep strains by using the above equations. The numerical calculation of the creep deformation was carried out using the above equations by the Runge–Kutta method. The instantaneous plastic strain and elastic strain were neglected in the present calculation.

4. Experimental procedure

Commercial carbon steels were used in the creep–rupture experiments in this study. Table I shows the chemical composition of the steels. The steel bars of 20 mm diameter and 80 mm length were heat treated to develop spherical cementite precipitate particles

and were then machined into creep–rupture test pieces of 5 mm diameter and 30 mm gauge length. Table II shows the heat treatments, the volume fraction, f, the average radius, a^*, and the interparticle spacing of cementite particles and the grain diameter of the specimens in the carbon steels. The heat-treated specimen of the S20C steel has almost the same average particle radius as that of the S80C steel, while almost no precipitates were observed in the specimen of pure iron. The grain diameter was almost the same in these specimens. Fig. 1 shows a scanning electron micrograph of the heat-treated specimen of the S80 steel. Spherical cementite particles are visible in the micrograph. Creep–rupture experiments were carried out using single lever-type creep–rupture equipment at 873 K in air.

5. Results of theoretical calculation and experimental results

5.1. Prediction of creep deformation

The numerical calculation was made on the basis of the micromechanics model for carbon steels containing cementite particles. The value of the rigidity, $\mu = \mu^* = 61\,600$ MPa and that of Poisson's ratio, $\nu = \nu^* = 0.34$ [16] were used in the numerical calculation at 873 K, because it is known that the elastic constants of ferrite are almost the same as those of cementite phase at room temperature [17]. The preliminary calculation revealed that the value of C for volume diffusion of iron atoms (in Equation 5) was at least 3×10^4 times larger than that of C for grain-boundary diffusion of iron atoms [12], if the volume diffusion coefficient of iron, $D_v = 4.13 \times 10^{-19}\,m^2\,s^{-1}$ [18], and the grain-boundary diffusion coefficient of iron, $D_{GB} = 4.51 \times 10^{-21}\,m^2\,s^{-1}$ at 873 K [19], the atomic volume of iron, $\Omega = 7.10 \times 10^{-6}\,m^3\,mol^{-1}$, and the grain-boundary thickness, $\delta \simeq 2b = 5.10 \times 10^{-10}$ m (b is the magnitude of the Burgers vector) [7], and the average particle radius in Table II were used in the calculation. Therefore, it was assumed in this study that the recovery process around cementite particles was controlled by volume diffusion of iron atoms. These physical constants (except D_{GB} and δ) were used in the present calculation. The following four θ_i parameters of the Θ projection obtained for ferrite steels in the previous study [5] were also used in this study.

$$\log_{10}\theta_1 = -1.344 + 7.889 \times 10^{-3}\,\sigma_e^I \quad (11a)$$

$$\log_{10}\theta_2 = -7.342 + 0.071\,86\,\sigma_e^I \quad (11b)$$

$$\log_{10}\theta_3 = -2.482 + 4.051 \times 10^{-3}\,\sigma_e^I \quad (11c)$$

$$\log_{10}\theta_4 = -7.287 + 0.068\,41\,\sigma_e^I \quad (11d)$$

Fig. 2 shows the calculated creep curves in the specimens of carbon steels containing spherical cementite particles under a stress of 49 MPa at 873 K. The creep curves of the carbon steels ($f = 0, f = 0.0342$ and $a^* = 4.37 \times 10^{-7}$ m) exhibit both transient creep and accelerated creep periods, whereas creep deformation seems to cease after long transient creep in the specimen containing cementite particles ($f = 0.0342$) when no diffusional recovery occurs. Fig. 3 shows the calculated and experimental creep curves in the specimens of carbon steels containing cementite particles tested under a stress of 49 MPa. The creep resistance of specimens increases with increasing volume fraction of cementite particles. There is a correlation between the calculated creep curves and the experimental ones in those steels, but the calculated values give smaller creep strains than the experimental ones near the

TABLE I Chemical composition (wt %) of the steels used in this study

Steels	C	Si	Mn	P	S	Fe
Pure iron	0.03	0.19	0.28	0.015	0.011	Bal.
S20C	0.22	0.22	0.45	0.016	0.018	Bal.
S80C	0.83	0.21	0.48	0.011	0.004	Bal.

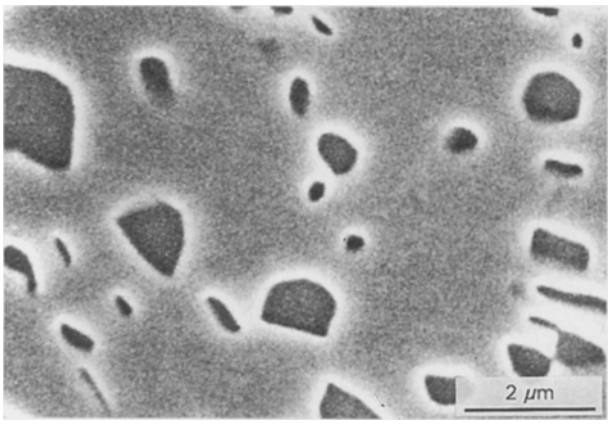

Figure 1 A scanning electron micrograph of the heat-treated specimen of the S80C steel.

TABLE II The volume fraction, the average particle radius and the average interparticle spacing of the cementite particles and the grain size in the heat-treated specimens of the steels

Steels	Heat treatments	Cementite particle			Grain diameter (10^{-6} m)
		Volume fraction, f	Particle radius, a^* (10^{-7} m)	Interparticle spacing, l (10^{-6} m)	
Pure iron	1323 K,7.2 ks → AC[a] → 973 K → AC	0.0	–	–	72
S20C	1423 K, 3.6 ks → AC + 973 K, 180 ks → AC	0.0342	4.37	2.18	72
S80C	1373 K, 3.6 ks → AC + 973 K, 180 ks → AC	0.136	3.82	1.90	78

[a] AC = air cooled.

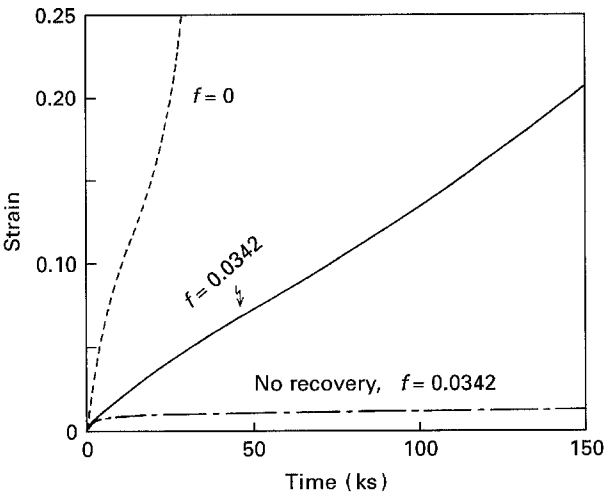

Figure 2 The calculated creep curves in the specimens of carbon steels containing spherical cementite particles under a stress of 49 MPa at 873 K (f = volume fraction of cementite particles).

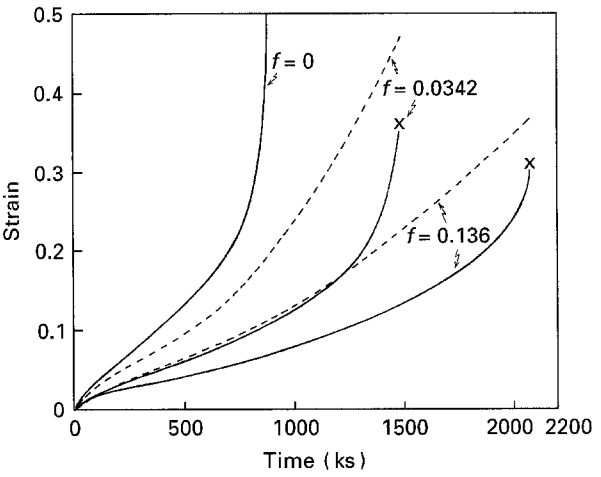

Figure 4 The (– – –) calculated and (——) experimental creep curves of the specimens of carbon steels containing cementite particles tested under a stress of 29.4 MPa at 873 K.

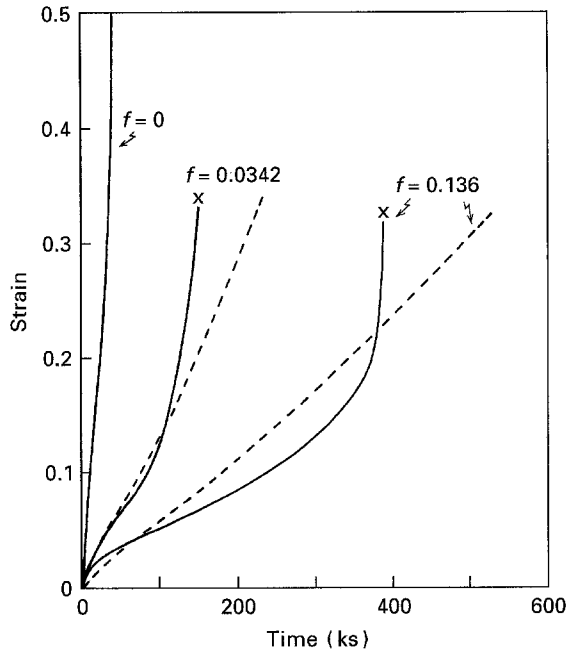

Figure 3 The (– – –) calculated and (——) experimental creep curves in the specimens of carbon steels containing cementite particles tested under a stress of 49 MPa at 873 K.

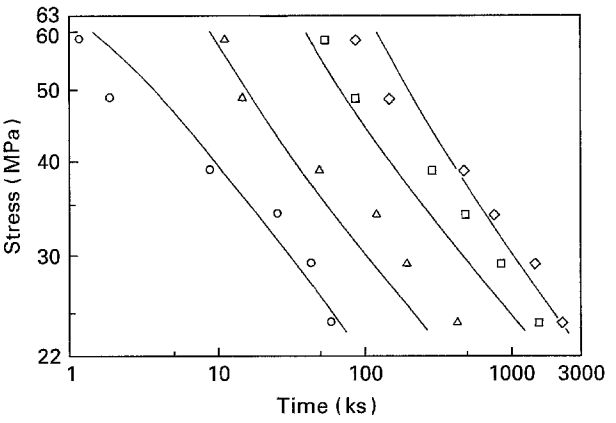

Figure 5 The relationship between the time to a given creep strain and the creep stress in the specimens containing cementite particles of $f = 0.0342$ during creep at 873 K. ε: (○) 0.01, (△) 0.03, (□) 0.10, (◇) 0.30, (——) calculated.

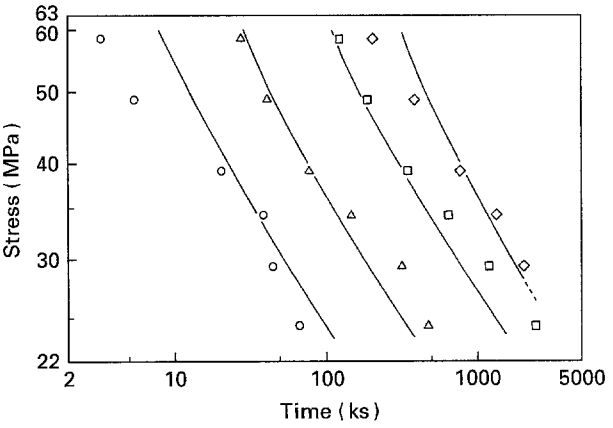

Figure 6 The relationship between the time to a given creep strain and the creep stress in the specimens containing cementite particles of $f = 0.136$ during creep at 873 K. For key, see Fig. 5.

rupture life. Fig. 4 shows the calculated and experimental creep curves in the specimens of carbon steels containing cementite particles tested under a stress of 29.4 MPa. The calculated creep strain is a little larger than the experimental one in both specimens of $f = 0.0342$ and 0.136, but there is a correlation between the shape of the calculated creep curves and that of the experimental ones, except around the fracture strain.

Fig. 5 shows the relationship between the time to a given creep strain and the creep stress in the specimens of $f = 0.0342$ of carbon steels during creep at 873 K. The stress dependence of the time to a given creep strain calculated on the micromechanics model agrees with that experimentally obtained in the creep strain range from 0.01–0.30, although the theoretical calculation gives a little longer time to 0.01 strain under the higher stresses. Fig. 6 shows the relationship between the time to a given creep strain and the creep stress in the specimens of $f = 0.136$ of carbon steels during creep at 873 K. The stress dependence of the time to a given creep strain is a little larger in the

specimens of $f = 0.136$ than in the specimens of $f = 0.0342$ in Fig. 5, and there is an agreement on the stress dependence of the time to a given creep strain between the calculated time and the experimental one, except for the smallest creep strain under the higher stresses. The instantaneous plastic strain and elastic strain were neglected in the present calculation. This may be the reason why there is a difference in the time to a given creep strain between the calculated values and the experimental ones under the higher stresses in these specimens.

5.2. Creep rate and equivalent stresses during creep

Fig. 7 shows the change in the creep rate with time in the specimens of $f = 0.0342$ during creep at 873 K. The experimental creep rate decreases at first rapidly and then gradually with time, and increases after showing a minimum value. The time dependence of the calculated creep rate shows an inverse sigmoidal shape and agrees with the experimental results, except in the very early stage of creep deformation under the lower stress (29.4 MPa) and the accelerated creep regime under the higher stress (49 MPa). Fig. 8 shows the change in the creep rate with time in specimens with

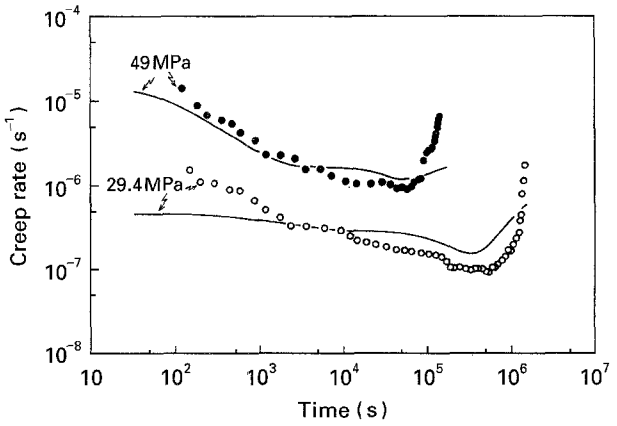

Figure 7 The change in the creep rate with time in the specimens containing cementite particles of $f = 0.0342$ during creep at 873 K. (○, ●) Experimental, (——) calculated.

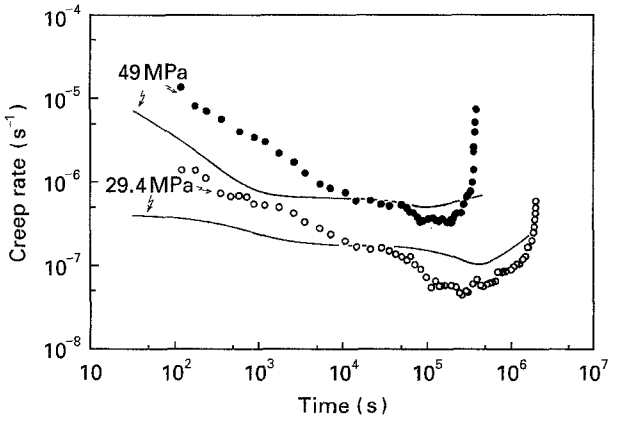

Figure 8 The change in the creep rate with time in the specimens containing cementite particles of $f = 0.136$ during creep at 873 K. (○, ●) Experimental, (——) calculated.

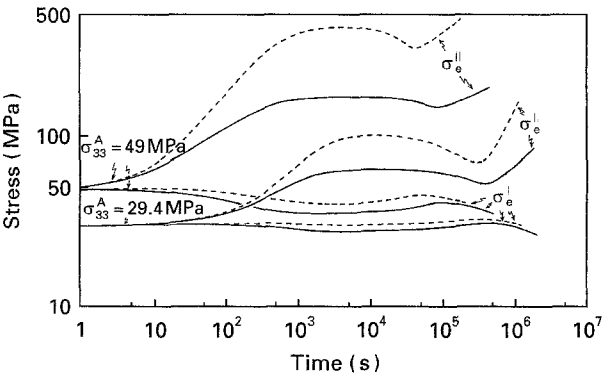

Figure 9 The change in the equivalent stress calculated for matrix, σ_e^I, and for the cementite particles, σ_e^{II}, in the specimens containing cementite particles during creep at 873 K. *f*: (——) 0.136, (– – –) 0.0342.

$f = 0.136$ during creep at 873 K. There is a correlation between the stress dependence of the calculated creep rate and that of the experimental one under both stresses of 29.4 and 49 MPa, although the change in the creep rate with time is somewhat larger in the experimental results.

Fig. 9 shows the change in the equivalent stress calculated for the matrix, σ_e^I, and for the cementite particles, σ_e^{II}, in the specimens of carbon steels during creep at 873 K. The equivalent stress in each phase is a function of the average internal stress and the external stress, σ^A_{33} (Equations 3 and 4). The time dependence of the equivalent stress shows a sigmoidal shape in the cementite particles and an inverse sigmoidal one in the matrix. The maximum value of the equivalent stress in the cementite particles is larger in the specimens of the smaller volume fraction of cementite phase under the higher creep stresses.

Thus, the creep deformation of carbon steels containing spherical cementite particles was simulated by the continuum mechanics model, in which the Θ projection was incorporated as the constitutive equation and the effects of diffusional recovery was taken into account. However, it is necessary to take the creep damage into account in the constitutive equation (for example, in the form of a damage function) in order to reasonably predict the creep deformation near the creep fracture.

6. Conclusion

A micromechanics model, in which work-hardening caused by second-phase particles and diffusional recovery were taken into account, was proposed for explaining the creep deformation of dispersion-strengthened metals in high-temperature creep. A constitutive equation of the Θ projection was used to describe the whole creep curves from the onset of loading to rupture. The results of the calculation based on the present model were compared with those of the experiments on the carbon steels containing spherical cementite particles. There was a correlation between the experimental creep curves and the calculated ones. The changes in the calculated creep strain and creep rate with time were also compared

with the experimental results on the carbon steels. The micromechanics model in this study was found to be able to simulate the creep curves of the dispersion-hardened metals, except near the fracture strain.

References

1. F. GAROFARO, "Fundamentals of creep and creep-rupture in metals", translated by M. Adachi (Maruzen, Tokyo, 1968) p. 5.
2. R. W. EVANS and B. WILSHIRE, "Creep of metals and alloys (The Institute of Metals, London, 1985) p. 193.
3. R. W. EVANS, P. J. SCHARNING and B. WILSHIRE, in "Creep behaviour of crystalline solids", edited by B. Wilshire and R. W. Evans (Pineridge Press, Swansea, 1985) Ch. 5, p. 201.
4. M. TANAKA, T. SAKAKI and H. IIZUKA, *Acta Metall. Mater.* **39** (1991) 1549.
5. M. TANAKA, *J. Mater. Sci.* **28** (1993) 2750.
6. G. S. ANSELL and J. WEERTMAN, *Trans. Met. Soc. AIME* **215** (1959) 838.
7. M. TANAKA and H. IZUKA, *J. Mater. Sci.* **21** (1986) 1932.
8. J. D. ESHELBY, *Proc. R. Soc.* **A241** (1957) 376.
9. T. MURA and T. MORI, "Micromechanics" (Baifukan, Tokyo, 1976) p. 23.
10. T. MURA, "Micromechanics of defects in solids" (Martinus Nijhoff, The Hague, 1982) p. 63.
11. T. MORI and K. TANAKA, *Acta Metall.* **21** (1973) 571.
12. K. TANAKA and T. MORI, *ibid.* **18** (1970) 931.
13. K. TANAKA, K. WAKASHIMA and T. MORI, *J. Mech. Phys. Solids* **21** (1973) 207.
14. T. MORI and H. TOKUSHIGE, *Acta Metall.* **25** (1977) 635.
15. K. MATSUURA, *ibid.* **29** (1981) 643.
16. *Idem*, "Elastic moduli of metallic materials" (Japan Society of Mechanical Engineers, Tokyo, 1980) p. 43.
17. T. HANABUSA, J. FUKURA and H. FUJIWARA, *Trans. Jpn Soc. Mech. Engr.* **35** (1968) 237.
18. W. HUME-ROTHERY, "The structures of alloys of iron" translated by K. Hirano (Kyoritsu Publishers, Tokyo, 1968) p. 284.
19. D. W. JAMES and G. M. LEAK, *Philos. Mag.* **12** (1965) 491.

Received 13 April
and accepted 13 October 1994